The Astronomical Journal, 128:1529–1540, 2004 October
© 2004. The American Astronomical Society. All rights reserved. Printed in U.S.A.

ULTRACOMPACT DWARF GALAXIES IN ABELL 1689: A PHOTOMETRIC STUDY WITH THE ADVANCED CAMERA FOR SURVEYS

S. Mieske,[1,2] L. Infante,[1] N. Benítez,[3] D. Coe,[3] J. P. Blakeslee,[3] K. Zekser,[3] H. C. Ford,[3] T. J. Broadhurst,[4] G. D. Illingworth,[5] G. F. Hartig,[6] M. Clampin,[7] D. R. Ardila,[3] F. Bartko,[8] R. J. Bouwens,[3] R. A. Brown,[6] C. J. Burrows,[6] E. S. Cheng,[9] N. J. G. Cross,[3] P. D. Feldman,[3] M. Franx,[10] D. A. Golimowski,[3] T. Goto,[3] C. Gronwall,[11] B. Holden,[5] N. Homeier,[3] R. A. Kimble,[7] J. E. Krist,[6] M. P. Lesser,[12] A. R. Martel,[3] F. Menanteau,[3] G. R. Meurer,[3] G. K. Miley,[10] M. Postman,[6] P. Rosati,[13] M. Sirianni,[6,14] W. B. Sparks,[6] H. D. Tran,[15] Z. I. Tsvetanov,[3] R. L. White,[6] and W. Zheng[3]

Received 2004 March 31; accepted 2004 June 25

ABSTRACT

The properties of ultracompact dwarf (UCD) galaxy candidates in Abell 1689 ($z = 0.183$) are investigated, based on deep high-resolution images from the *Hubble Space Telescope* Advanced Camera for Surveys. A UCD candidate has to be unresolved, have $i < 28$ mag ($M_V < -11.5$ mag), and satisfy color limits derived from Bayesian photometric redshifts. We find 160 UCD candidates with 22 mag $< i < 28$ mag. We estimate that about 100 of these are cluster members, based on their spatial distribution and photometric redshifts. For $i \gtrsim 26.8$ mag, the radial and luminosity distribution of the UCD candidates can be explained well by Abell 1689's globular cluster (GC) system. For $i \lesssim 26.8$ mag, there is an overpopulation of 15 ± 5 UCD candidates with respect to the GC luminosity function. For $i \lesssim 26$ mag, the radial distribution of UCD candidates is more consistent with the dwarf galaxy population than with the GC system of Abell 1689. The UCD candidates follow a color-magnitude trend with a slope similar to that of Abell 1689's genuine dwarf galaxy population, but shifted fainter by about 2–3 mag. Two of the three brightest UCD candidates ($M_V \simeq -17$ mag) are slightly resolved. At the distance of Abell 1689, these two objects would have King profile core radii of $\simeq$35 pc and $r_{\rm eff} \simeq 300$ pc, implying luminosities and sizes 2–3 times those of M32's bulge. Additional photometric redshifts obtained with late-type stellar and elliptical galaxy templates support the assignment of these two resolved sources to Abell 1689 but also allow for up to four foreground stars among the six brightest UCD candidates. Our findings imply that in Abell 1689 there are $\geq$10 UCDs with $M_V < -12.7$ mag, probably created by stripping "normal" dwarf or spiral galaxies. Compared with the UCDs in the Fornax Cluster—the location of their original discovery—they are brighter, larger, and have colors closer to normal dwarf galaxies. This suggests that they may be in an intermediate stage of the stripping process. Checking the photometric redshifts of the brightest UCD candidates with spectroscopy would be the next step to definitely confirm the existence of UCDs in Abell 1689.

Key words: galaxies: clusters: individual (Abell 1689) — galaxies: dwarf — galaxies: fundamental parameters — galaxies: nuclei — globular clusters: general

1. INTRODUCTION

1.1. *Discovery of UCDs*

Recently, Drinkwater et al. (2000, 2003) reported on the discovery of seven ultracompact dwarf galaxies (UCDs) in the Fornax Cluster. These objects are very luminous star clusters in the magnitude range $-13.4 < M_V < -12$, i.e., about 1–2 mag brighter than ω Centauri. Three different origins for the UCDs are under discussion: (1) that they are the brightest globular clusters of very rich globular cluster systems (GCSs), such as those in in NGC 1399 (Mieske et al. 2002; Dirsch et al. 2003); (2) that they are the remnant nuclei of stripped dwarf galaxies that have lost their outer parts in the course of tidal interaction with the Fornax Cluster's potential (Bekki et al. 2003; Mieske et al. 2004); (3) that they are formed from the amalgamation of stellar superclusters (SSCs) in collisions between gas-rich galaxies (Fellhauer & Kroupa 2002; Kroupa 1998; Maraston et al. 2004).

These possibilities are discussed in more detail in Mieske et al. (2004). It is found that in Fornax there are 12 bright compact objects with -13.4 mag $< M_V < -11.4$ mag, including the UCDs. Applying an incompleteness correction raises this number to 14. The bright compact objects follow a color-magnitude relation in $V-I$ with a slope very similar to that of Fornax dE's (Hilker et al. 2003), but shifted about 0.2 mag redward. In addition, they appear to be separated from

[1] Departamento de Astronomía y Astrofísica, Pontificia Universidad Católica de Chile, Casilla 306, Santiago 22, Chile; linfante@astro.puc.cl.
[2] Sternwarte der Universität Bonn, Auf dem Hügel 71, D-53121 Bonn, Germany; smieske@astro.uni-bonn.de.
[3] Department of Physics and Astronomy, Johns Hopkins University, 3400 North Charles Street, Baltimore, MD 21218.
[4] Racah Institute of Physics, Hebrew University, 91904 Jerusalem, Israel.
[5] UCO/Lick Observatory, University of California, Santa Cruz, 1156 High Street, Santa Cruz, CA 95064.
[6] Space Telescope Science Institute, 3700 San Martin Drive, Baltimore, MD 21218.
[7] NASA Goddard Space Flight Center, Code 681, Greenbelt, MD 20771.
[8] Bartko Science and Technology, 14520 Akron Street, Brighton, CO 80602.
[9] Conceptual Analytics, LLC, 8209 Woburn Abbey Road, Glenn Dale, MD 20769.
[10] Sterrewacht Leiden, Postbus 9513, NL-2300 RA Leiden, Netherlands.
[11] Department of Astronomy and Astrophysics, 525 Davey Laboratory, Pennsylvania State University, University Park, PA 16802.
[12] Steward Observatory, University of Arizona, 933 North Cherry Avenue, Tucson, AZ 85721.
[13] European Southern Observatory, Karl-Schwarzschild-Strasse 2, D-85748 Garching, Germany.
[14] Research and Scientific Support Department, European Space Agency.
[15] W. M. Keck Observatory, 65-1120 Mamalahoa Highway, Kamuela, HI 96743.

the fainter compact Fornax members ($M_V > -11.4$ mag) in radial velocity and are spatially distributed in a more extended fashion. The properties of the faint compact Fornax members are consistent with the globular cluster system of NGC 1399. The properties of bright compact Fornax members seem to be different from those of normal globular clusters. They are consistent with the threshing scenario of Bekki et al. (2003), who propose tidal stripping of nucleated dwarf galaxies as a source of bright compact cluster members. Their properties are also consistent with the supercluster scenario as proposed by Fellhauer & Kroupa (2002), suggesting for the first time a color-magnitude relation for bright globular clusters, if true.

If UCDs are bright compact stellar systems distinct from globular clusters, the results of Mieske et al. (2004) then show that UCDs in Fornax populate the color-magnitude range -13.4 mag $< M_V < -11.4$ mag and 1.0 mag $< V-I <$ 1.30 mag, extending the discoveries by Drinkwater et al. (2003) to fainter limits.

1.2. *UCDs in Abell 1689?*

In the case of Abell 1689 ($z = 0.183$; Tyson & Fischer 1995), one of the most massive known galaxy clusters ($M \simeq 0.5$–$2 \times 10^{15}\ M_{\odot}$, $M/L \simeq 400$, and $r_s \simeq 350$ kpc; see the lensing studies by Broadhurst et al. 2004 and King et al. 2002), it is very interesting to estimate the number of UCD candidates. Is Fornax a special case, or are UCDs a more general phenomenon? A consequence of the latter possibility would be that entire tidal disruption of fainter dwarf galaxies might occur in many clusters and could therefore partially cause the "missing satellite" problem (Moore et al. 1999; Klypin et al. 1999). Detailed numerical simulations regarding this issue might become necessary. However, it is also necessary to address the extent to which the number of UCD candidates can be accounted for by the very rich GCS of Abell 1689 (Blakeslee et al. 2004). As Abell 1689 consists of several subclusters in radial velocity (Teague et al. 1990; Girardi et al.1997), there is the possibility of merger events having occurred in the recent past. This might cause the creation of SSCs (Fellhauer & Kroupa 2002) and therefore also contribute to the number of UCDs. Abell 1689 has a mean redshift of $z = 0.1832$ (from NED). Assuming $H_0 = 70$ km s^{-1} Mpc^{-1}, $\Omega_M = 0.3$, and $\Omega_\Lambda = 0.7$, the corresponding distance modulus ($m - M$) is 39.74 mag. Taking into account the k-correction, which is about 0.3 mag for V at the redshift of Abell 1689, we look for objects in the apparent magnitude range $26.65 < V < 28.65$, a task that requires very deep imaging.

The aim of this paper is to estimate the number of UCD candidates in Abell 1689 and to investigate their distribution in luminosity, color, and space using deep *Hubble Space Telescope* Advanced Camera for Surveys (ACS) imaging data. Section 2 describes the ACS data. In § 3, the properties of UCD candidates are investigated. In § 4, the findings are discussed. Section 5 presents the conclusions.

2. THE DATA

The photometric data used in this paper are extracted from deep ACS images of Abell 1689, obtained from the ACS Guaranteed Time Observations deep imaging cluster Wide Field Camera (WFC) data in 2002 June. The WFC covers a field of view of $202'' \times 202''$, with $0''.05$ pixels. The data are presented in more detail in Broadhurst et al. (2004). A total of 20 orbits were taken in the four passbands F475W (g), F625W (r), F775W (i), and F850L (z), corresponding to the Sloan Digital Sky Survey (SDSS) $g'r'i'z'$ filters. The point-spread function (PSF) FWHM is $0''.10$–$0''.11$, or about 2 pixels, in each filter. The limiting magnitude for detecting point sources with at least 5 pixels above 1.5 σ is $i \simeq 28.5$ mag. The faint limit of the UCD magnitude regime of $V = 28.65$ corresponds to $i \simeq 28.0$ mag (Fukugita et al. 1996).

At the distance of Abell 1689, $0''.1 = 310$ pc. All UCDs in Fornax have scale lengths of 10–20 pc. Their analogs are hence detectable but unresolved on the ACS images of Abell 1689.

Detection and analysis of unresolved sources was done using SExtractor (Bertin & Arnouts 1996) on the ACS images, where all bright galaxies were previously subtracted (see Zekser et al. 2004). SExtractor was run in dual mode, involving first detecting sources on the detection image (inverse-variance–weighted average of the four passband images; see Benítez et al. 2004) and then carrying out their analysis on each single passband. Sources were defined as unresolved when the SExtractor star-classifier values were larger than 0.6. Magnitudes were determined from aperture photometry.

Using the technique outlined by Benítez (2000), Coe et al. (2004) provide Bayesian photometric redshifts for almost 2000 sources in Abell 1689. The ACS *griz* data were complemented by VLT optical and infrared photometry. In this paper these photometric redshifts are used to help distinguish unresolved cluster members from background galaxies. The analysis of the resolved sources, and thereby of the normal dwarf galaxy population in Abell 1689, is presented in a separate paper (Infante et al. 2004).

3. PHOTOMETRIC SELECTION AND PROPERTIES OF UCD CANDIDATES IN ABELL 1689

In this paper two different methods to separate cluster members from background galaxies are applied: first is a color selection applied to unresolved objects, based on and complemented by photometric redshifts, and, second, a statistical background subtraction using the radial density distribution of the color-selected objects. The background contaminations derived from both methods are compared. To search for UCD candidates, a circular region of $92''$ (285 kpc) radius centered on the brightest cluster galaxy was analyzed. This was the largest possible circular region imaged entirely by ACS. See the paper by Broadhurst et al. (2004) for the optical ACS image of the cluster.

3.1. *Color Selection and Background Contamination from Photometric Redshifts*

The left panels of Figure 1 show two color-magnitude diagrams (CMDs) in $g-i$ and $r-z$, respectively, of all unresolved sources in the ACS field of Abell 1689. The faint magnitude limit for UCD candidates is $i = 28$ mag. To help define color selection windows for UCD candidates, photometric redshifts $z_{\rm phot}$ from Coe et al. (2004) are indicated in the right panels of Figure 1 to separate cluster member candidates from background galaxies (*circles*, $z_{\rm phot} \leq 0.5$; *crosses*, $z_{\rm phot} > 0.5$). In addition, the color windows in $g-i$ and $r-z$ corresponding to the VI colors of UCDs in Fornax are also indicated. The color transformations were calculated using the calibrations of the ACS bandpasses described in Sirianni et al. (2004), including k-corrections.

The $z_{\rm phot} = 0.5$ limit between cluster and background objects is clear from inspecting Figure 2. It shows a histogram of the photometric redshift distribution of sources in the field of view of the Abell 1689 ACS image (Coe et al. 2004). Apart from the most probable photometric redshift $z_{\rm med}$, also shown are the smallest and largest possible redshifts, $z_{\rm min}$ and $z_{\rm max}$ (2 σ). Apparently, there is a pronounced peak around

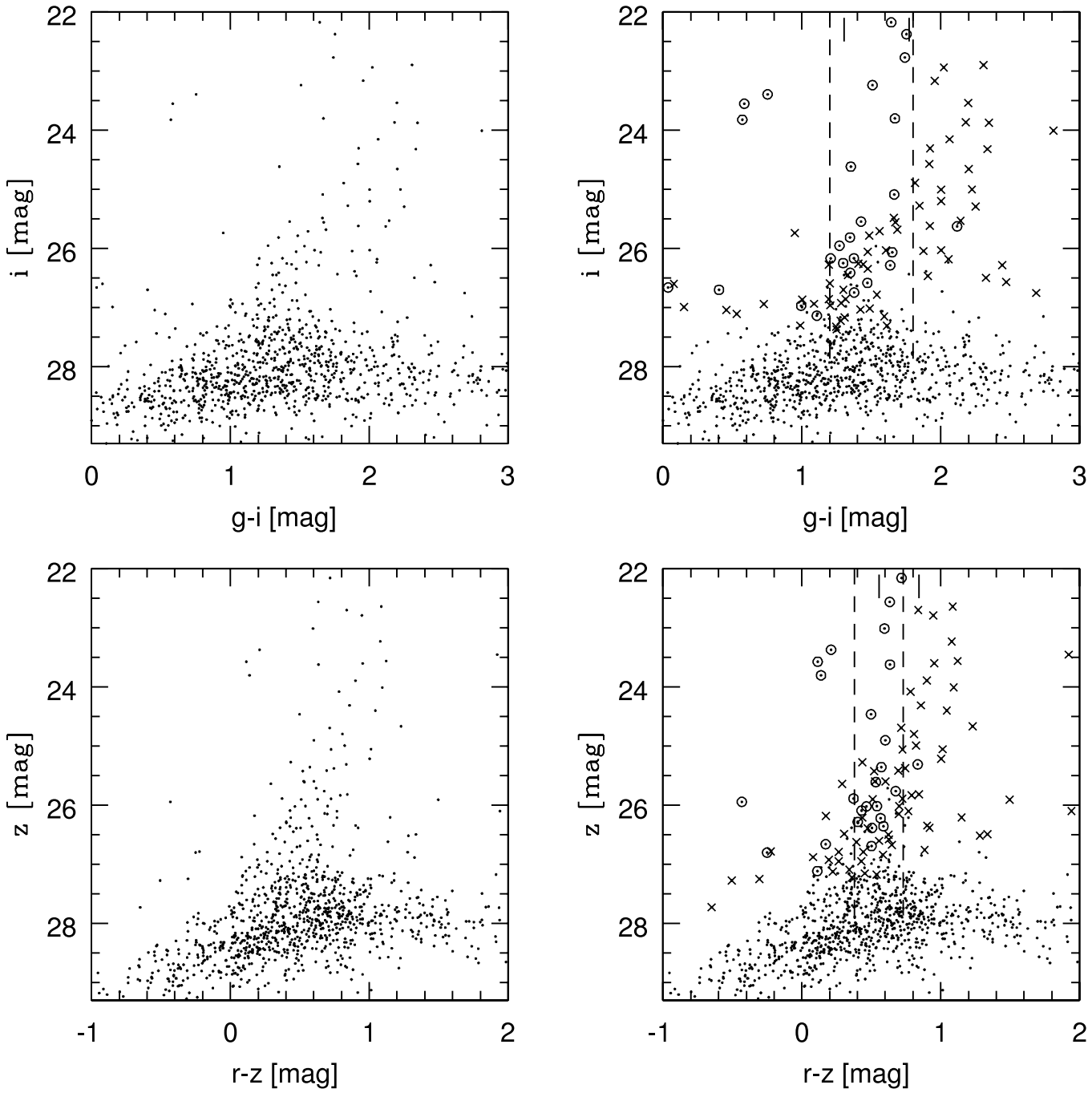

FIG. 1.—*Top left*: CMD in i and $g-i$ of all unresolved sources in the central 92″ (285 kpc) of Abell 1689. *Top right*: Dots as plotted to the left; circles indicate objects with photometric redshift $z_{\rm phot} \leq 0.5$ (taken from Broadhurst et al. 2004 and Coe et al. 2004), and crosses objects with $z_{\rm phot} > 0.5$. Vertical ticks at the top indicate the blue and red color limit of UCDs from Fornax (Mieske et al. 2004), transformed from *VI* to *gi* using the calibrations of the ACS bandpasses described in Sirianni et al. (2004). Dashed vertical lines indicate the color window finally adopted in $g-i$ for UCD candidates in Abell 1689, extending slightly more blueward compared with the transformed UCD colors in Fornax. *Bottom*: Same as top, but in z and $r-z$. The color selection window is shifted about 0.15 mag blueward compared with the transformed UCD colors.

$z_{\rm med} = 0.25$, corresponding roughly to the redshift of Abell 1689. The distributions of $z_{\rm min}$ and $z_{\rm max}$ show, however, that photometric redshift values much closer to 0 and also up to about 0.5 are possible for objects whose $z_{\rm med} \simeq 0.25$. We therefore adopt a limit of $z_{\rm med} \leq 0.5$ for cluster membership assignment based on photometric redshifts, providing an upper limit on the number of cluster members. The spectroscopic survey of Abell 1689 by Duc et al. (2002), in particular Figure 1 in that paper, indicates that the redshift space behind the cluster is very sparsely populated until at least $z = 1$. The ratio of background to cluster galaxies is only a few percent. The same holds for the number of foreground galaxies. Therefore, the limit $z_{\rm med} < 0.5$ should yield a fair estimate of the real number of cluster members. It is important to note here that the use of photometric redshifts helps in defining the color window only for $i \leq 27$ UCD candidates, as fainter than that no photometric redshifts are available.

In $g-i$, the limit between $z_{\rm phot} \leq 0.5$ and $z_{\rm phot} > 0.5$ is well defined at about $g-i = 1.8$ mag. Hence, this color is adopted as the red limit for UCD candidates. The red color limit of UCDs

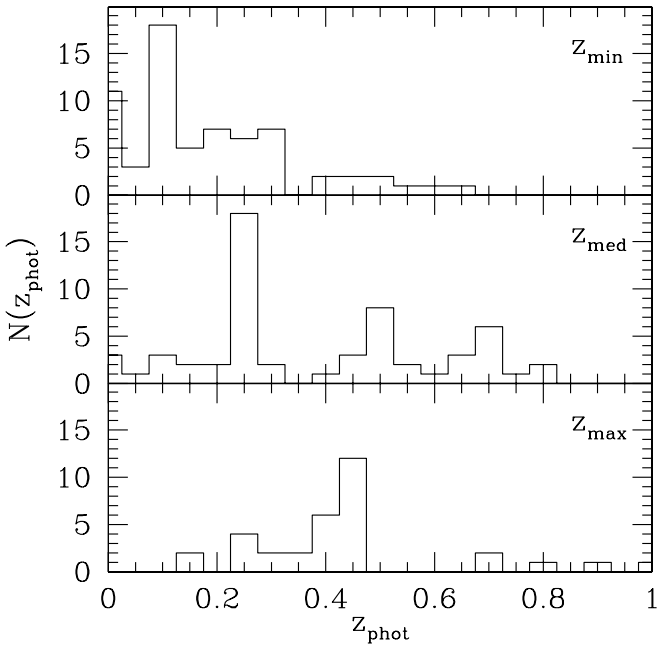

FIG. 2.—Histograms of photometric redshifts of unresolved sources in Abell 1689, taken from Coe et al. (2004). The values $z_{\rm min}$, $z_{\rm med}$, and $z_{\rm max}$ refer to the minimum (2 σ), medium, and maximum (2 σ) photometric redshifts, respectively, obtained with the Bayesian approach described in Benítez (2000).

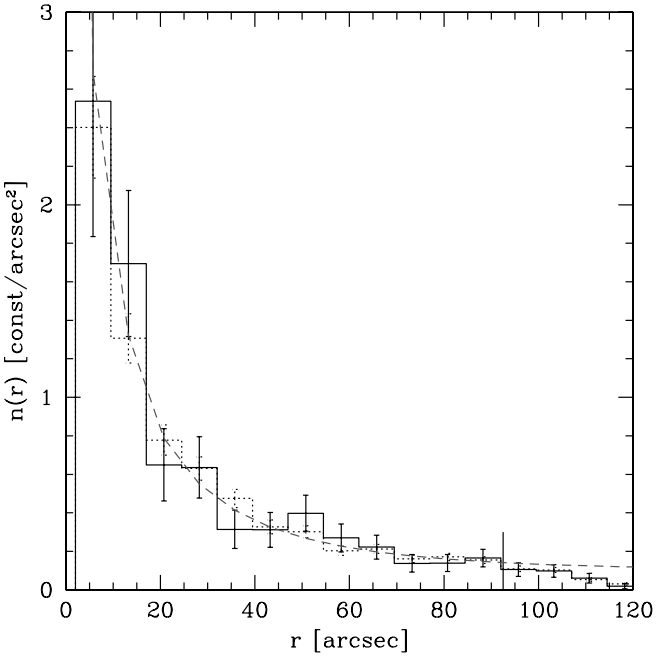

FIG. 3.—Surface density distribution of unresolved sources in Abell 1689 (arbitrary scale) plotted vs. projected distance r to the central galaxy. *Dotted histogram*, all unresolved sources, the majority of which are Abell 1689 globular clusters (Blakeslee et al. 2004); *solid histogram*, UCD candidates. Both histograms are scaled to the total number of objects included times an arbitrary factor. The tick at 92″ marks the image limit. The dashed line indicates the fit to the solid histogram, consisting of a Sérsic profile plus the background density corrected for lensing magnification effects (see text for further details).

in Fornax is $V-I = 1.30$ mag. Using the ACS bandpass calibrations from Sirianni et al. (2004), this corresponds to $g-i = 1.77$ mag, almost identical to the adopted red color limit based on photometric redshifts. The blue color limit is adopted as $g-i = 1.2$ mag, as this is the approximate blue limit of point sources with reliable colors. The objects bluer than that are dominated by fainter sources with large color errors (see Fig. 1). In total, this yields the color window 1.2 mag $< g-i <$1.8 mag for UCD candidates. In $r-z$, analogous considerations yield a color window 0.38 mag $< r-z <$ 0.73 mag. The color selection windows are quadratically broadened by the object's color error for each object. The final selection criteria for UCD candidates are SExtractor star-classifier values larger than 0.6, $i < 28$ mag, 1.2 mag $< g-i <$ 1.8 mag, 0.38 mag $< r-z <$ 0.73 mag, and distance from the cluster center $r < 92''$.

For objects with photometric redshift that fall into the color selection windows, the background contamination can be estimated. There are 33 objects with $z_{\rm phot}$ in the color window, spanning the magnitude range $22 < i < 27.5$. Out of these, 17 have $z_{\rm phot} \leq 0.5$. This corresponds to a background contamination of 48.5% ± 12%.

3.2. *Background Contamination from Radial Density Distribution*

Figure 3 shows the surface density distribution of the UCD candidates in Abell 1689 as selected in the previous section, together with the distribution of all unresolved sources. In total, there are 160 UCD candidates within a radius of 92″, which is the distance from the cluster center to the image limit. The UCD candidates are strongly clustered, with their distribution agreeing very well with that of all unresolved sources. Note that the latter objects are dominated by Abell 1689's globular cluster system (Blakeslee et al. 2004).

The total number of 160 UCD candidates in Abell 1689 must be corrected for the contribution of background number counts. To do so, a Sérsic profile plus a radius-dependent background density was fitted to the surface density distribution of UCD candidates. Note that a Sérsic profile yielded a better fit than a power law. The inclusion of a radius-dependent background density takes into account the fact that the lens magnification changes the number density of observed background objects. Following Blakeslee (1999) and King et al. (2002), we adopt a simple isothermal profile for the magnification $\mu(\theta)$, yielding

$$\mu(\theta) = [1 - (\theta/\theta_{\rm E})^{-1}]^{-1} \ . \qquad (1)$$

We adopt $\theta_{\rm E} = 36''$ as the Einstein radius of Abell 1689, which is the mean of the values derived by King et al. (2002) from weak lensing and Broadhurst et al. (2004) from strong lensing. Given the undistorted background number density $N_{\rm bg}(m)$, it holds for the observed background number density $N^*_{\rm bg}(m, \theta)$ that

$$N^*_{\rm bg}(m, \theta) = \frac{1}{\mu(\theta)} N_{\rm bg}[m + 2.5 \log \mu(\theta)]. \qquad (2)$$

Assuming a power-law distribution $N_{\rm bg}(m) \propto 10^{m\beta}$ with $\beta = 0.32$ (Benítez et al. 2004) and applying equations (6) and (7) of Blakeslee (1999) yields

$$N^*_{\rm bg}(m, \theta) = N_{\rm bg}(m)[1 - (\theta/\theta_{\rm E})^{-1}]^{0.2} \ . \qquad (3)$$

The fact that the exponent is positive shows that the decrease in surface density of background sources dominates over the number-count increase of detectable objects due to the magnification. In other words, the density of background objects decreases toward the cluster center, in this case by about 10% as compared with a constant, radially independent background density.

The result of the fit is that the total background contamination for $r < 92''$ is 26% ± 22%. This means that taking into account the effect of lensing on the number density of background objects increases the number of cluster members by about 3%. The error of the background contamination is considerable because of the fact that four variables (central surface density, scale radius, Sérsic index, background density) are fitted at the same time. When fixing the fitted values for scale radius and Sérsic index, the error of the background contamination decreases from 22% to 13%. In either case, the result of 26% ± 23% (or ±13%) agrees to within its errors with the background contamination of 48.5% ± 12% estimated from photometric redshifts in the previous section. Adopting the mean of both values, i.e., 37%, about 100 out of the 160 UCD candidates should be cluster members. This means that there are about 7 times more objects in the color-magnitude range of UCDs than in Fornax, where 14 UCDs are found (as Mieske et al. 2004). A further discussion of this issue is given in §§ 3.5 and 4.

3.3. *Luminosity Distribution of UCD Candidates*

Figure 4 shows the luminosity distribution of UCD candidates in Abell 1689. The counts have been corrected for the contribution of background sources using the value of 37% contamination derived in § 3.2. Gaussian globular cluster luminosity functions (GCLFs) with widths $\sigma = 1.2$, 1.3, 1.4, and 1.5 mag all match reasonably well the number counts for $i \leq 26.8$ mag ($M_V \simeq -12.7$ mag), resulting in a total number $N_{\rm glob}$ between 135,400 for $\sigma = 1.2$ mag and 17,100 for $\sigma = 1.5$ mag. The χ^2 value of the fit is best for $\sigma = 1.4$ mag, consistent with what is usually found for GC systems (Kundu & Whitmore 2001). Note that, unlike for the Fornax case, where the GC system of NGC 1399 has been investigated beyond the turnover magnitude (TOM), this is not possible for Abell 1689. In i, the TOM lies at about $i \simeq 31.8$ mag, far beyond the reach of even the ACS. This is why the total number of GCs can be restricted only poorly with the existing data. Crowding is not a significant effect: random position simulations of globular clusters belonging to a GCS with TOM $i = 31.8$ mag, $\sigma = 1.4$ mag, and $N_{\rm glob} = 50{,}000$ show that only 1.5% of the clusters with $i < 29.5$ mag—1 mag fainter than the completeness limit—are less than 2 FWHM away from their next neighbor.

For magnitudes brighter than $i \simeq 26.8$ ($M_V \simeq -12.7$), there is an overpopulation of UCD candidates with respect to any of the adopted Gaussian LFs. The number of GCs with ≤ 26.8 mag expected from the GCLF with width $\sigma = 1.4$ mag is 4.8, while the number of candidate UCDs is 20.9. The two values are inconsistent at the 3.5 σ level. Note that the noninteger numbers are caused by the statistical background decontamination.

The faint magnitude limit of $M_V \simeq -12.7$ for the overpopulation is about 1 mag brighter than the faint magnitude limit of UCDs in Fornax. This might indicate that the objects equivalent to UCDs in Fornax are brighter in Abell 1689. Before that conclusion is made, it must be clarified whether the several 10^4 to 10^5 GCs needed to explain the number counts for $i > 26.8$ mag can at all be contained in the GCS of Abell 1689. Assuming $S_N = 6$, a value found, for example, for the Fornax Cluster's central galaxy NGC 1399 (Dirsch et al. 2003), the total number of GCs belonging to the 10 brightest cluster galaxies in Abell 1689 (-23.1 mag $< M_V < -21.4$ mag; Zekser et al. 2004) is 44,500, being on the order of the values found above. Thus, it is not necessary to introduce objects other than genuine GCs as contributing to the number counts for $i \geq 26.8$ mag.

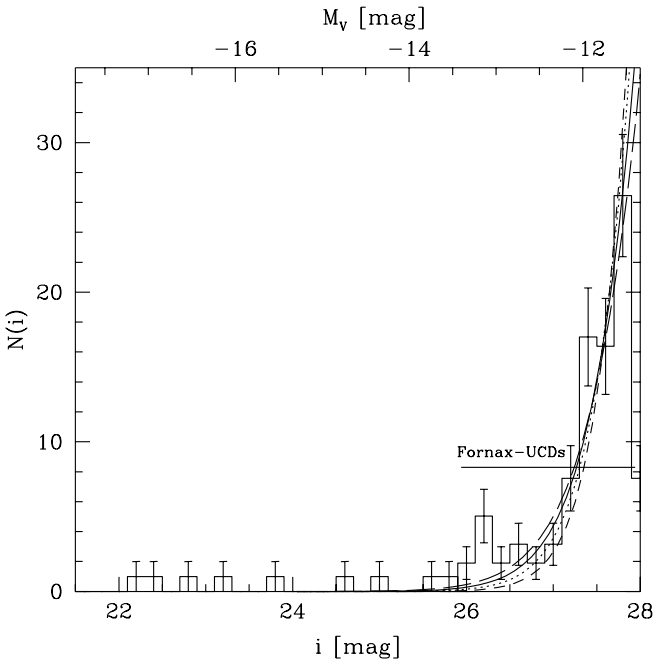

FIG. 4.—Luminosity distribution of UCD candidates in Abell 1689 within $92''$ of the cluster center. Note that for $i > 26$ mag, these are the number counts of all UCD candidates multiplied by $1 - 0.37$, with 0.37 being the background contamination fraction found in § 3. For $i < 26$ mag, all UCD candidates have a photometric redshift available. Therefore, instead of making a statistical background decontamination, only the UCD candidates with $z_{\rm phot} < 0.5$ are included in the luminosity distribution (see § 3). The magnitude range of the UCDs in Fornax is indicated by the horizontal tick. The long-dashed, solid, dotted, and short-dashed lines correspond to a Gaussian GCLF at Abell 1689's distance with $\sigma = 1.5$, 1.4, 1.3, and 1.2 mag, respectively. The fitted respective total number of GCs is $N_{\rm glob} = 17{,}100$, 30,100, 59,300, and 135,400. The fit with $\sigma = 1.4$ mag and corresponding $N_{\rm glob} = 30{,}100$ has the lowest χ^2.

Therefore, based on the magnitude distribution, for $i \leq 26.8$ mag we find evidence for an overpopulation with respect to the GCLF, while for $i \geq 26.8$ mag the number counts are consistent with a regularly rich GCS following a Gaussian LF.

3.4. *Color Distribution of UCD Candidates versus Normal Dwarf Galaxies*

To investigate the subpopulation of UCD candidates that constitutes an overpopulation with respect to Abell 1689's GCLF, Figures 5 and 6 show CMDs of UCD candidates with $i < 27$ mag in $g-i$ and $r-z$, respectively. The colors of resolved objects with $z_{\rm phot} < 0.5$ are given to illustrate the location of the color-magnitude sequence for dwarf galaxies in the cluster. A detailed paper on these resolved objects is in preparation (Infante et al. 2004).

The following main features are extracted from the CMDs:

1. UCD candidates extend to much brighter magnitudes than in Fornax. The brightest UCD candidate in Abell 1689 has $M_V \simeq -17$ mag, about as bright as the compact elliptical galaxy M32 (Mateo 1998).

2. UCD candidates and dwarf galaxies follow color-magnitude trends in the sense that color becomes redder with growing luminosity. For the UCD candidates, the slope is -0.069 ± 0.006 for $g-i$ and -0.027 ± 0.005 for $r-z$.

3. UCD candidates are redder than dwarf galaxies of the same brightness, a behavior that is more pronounced in $g-i$ (about 0.3 mag difference) than in $r-z$ (between 0.0 and 0.2 mag difference).

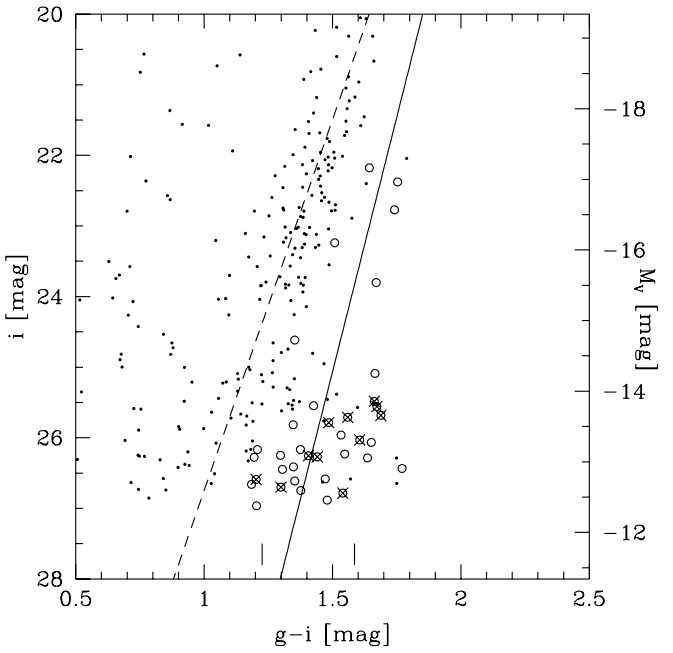

FIG. 5.—CMD in (i, $g-i$) of UCD candidates with $i < 27$ mag, indicated as circles, and resolved objects in Abell 1689 with $z_{\rm phot} < 0.5$ taken from Infante et al. (2004), indicated as dots. Crosses mark unresolved UCD candidates with $z_{\rm phot} > 0.5$. The lines indicate the fitted color-magnitude relation to the resolved sources (*dashed line*) and the UCD candidates (*solid line*). Note that the brightest UCD in Fornax has $M_V = -13.4$ mag, several magnitudes fainter than found here. The vertical ticks denote the average position of the blue and red peaks of the GCLF (Kundu & Whitmore 2001).

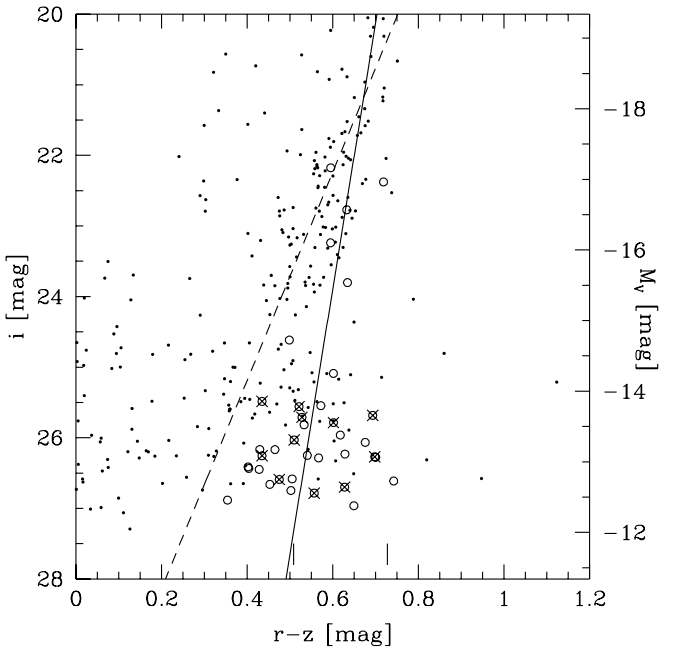

FIG. 6.—Same as Fig. 5, but in (i, $r-z$).

4. UCD candidates are more consistent with the red than the blue peak of the bimodal GC color distribution.

Features 2, 3, and 4 are qualitatively consistent with observations of UCDs in the Fornax Cluster (Mieske et al. 2004). The interpretation is that UCDs are created by tidally disrupting nucleated dwarf galaxies (dE,N's), which are stripped by repeated passages through the cluster's potential well of all but the nuclear part and hence become "ultracompact" (Bekki et al. 2003). In a CMD a dE,N moves toward fainter magnitudes at unchanged color. The final products of this threshing procedure, namely, the UCDs, then define a color-magnitude relation with similar slope to that of dE's, but shifted redward. The most interesting feature is that the Abell 1689 UCD candidates reach the luminosity of very bright "normal" dwarf galaxies: they extend to $M_V \simeq -17$ mag, while the magnitude limit between dwarf and giant galaxies is only 1–2 mag brighter (Hilker et al. 2003). This could mean that at least in the case of the brightest UCD candidates, we are seeing objects in the transition phase between dE,N's and UCDs, as a magnitude difference of about 4 mag between dE,N's and UCDs is expected (Bekki et al. 2003).

The idea that the brightest UCD candidates are just the smallest genuine dE's of a continuous distribution is another possible explanation for our findings. However, Figure 7 shows that the size distribution of all (unresolved and resolved) objects in the magnitude range $22 < i < 24$ is not consistent with that assumption. The size distribution of resolved sources has a sharp lower cutoff at about 0.″2 FWHM, twice as large as the FWHM of the UCD candidates. This dichotomy is also present in the (i, $g-i$) CMD in Figure 5, where the UCDs are well separated from the resolved objects.

In § 4, the implications of our findings are discussed further.

3.5. *Radial Distribution of UCD Candidates versus Normal Dwarf Galaxies*

Figure 8 shows the cumulative radial distribution of UCD candidates and dE candidates in Abell 1689, with the latter data taken from Infante et al. (2004). The sample of UCD candidates is split into three overlapping subsamples: $i < 27$ mag (UCD_1 hereafter), $i < 26$ mag (UCD_2), and $i < 25$ mag (UCD_3). In addition, the distribution of unresolved objects

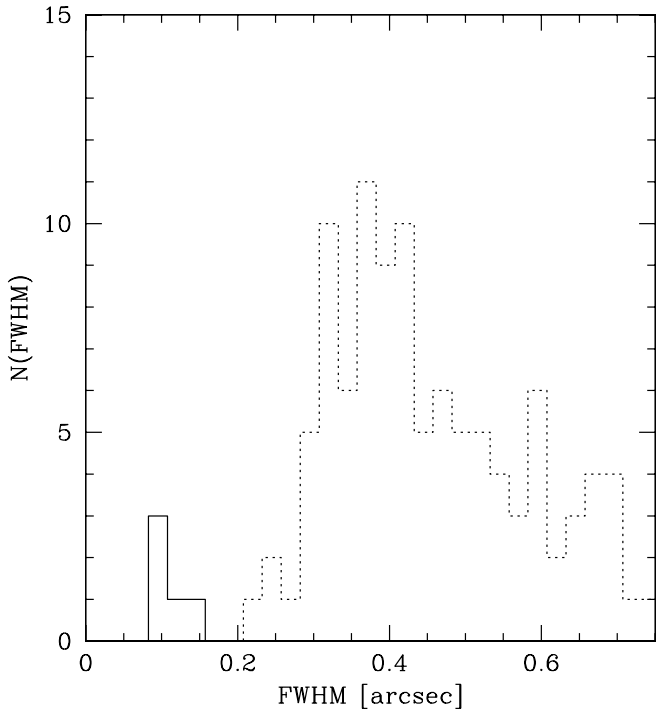

FIG. 7.—Size distribution of objects from Fig. 5 with 22 mag $< i <$ 24 mag. *Solid histogram*, UCD candidates; *dotted histogram*, resolved objects, taken from Infante et al. (2004).

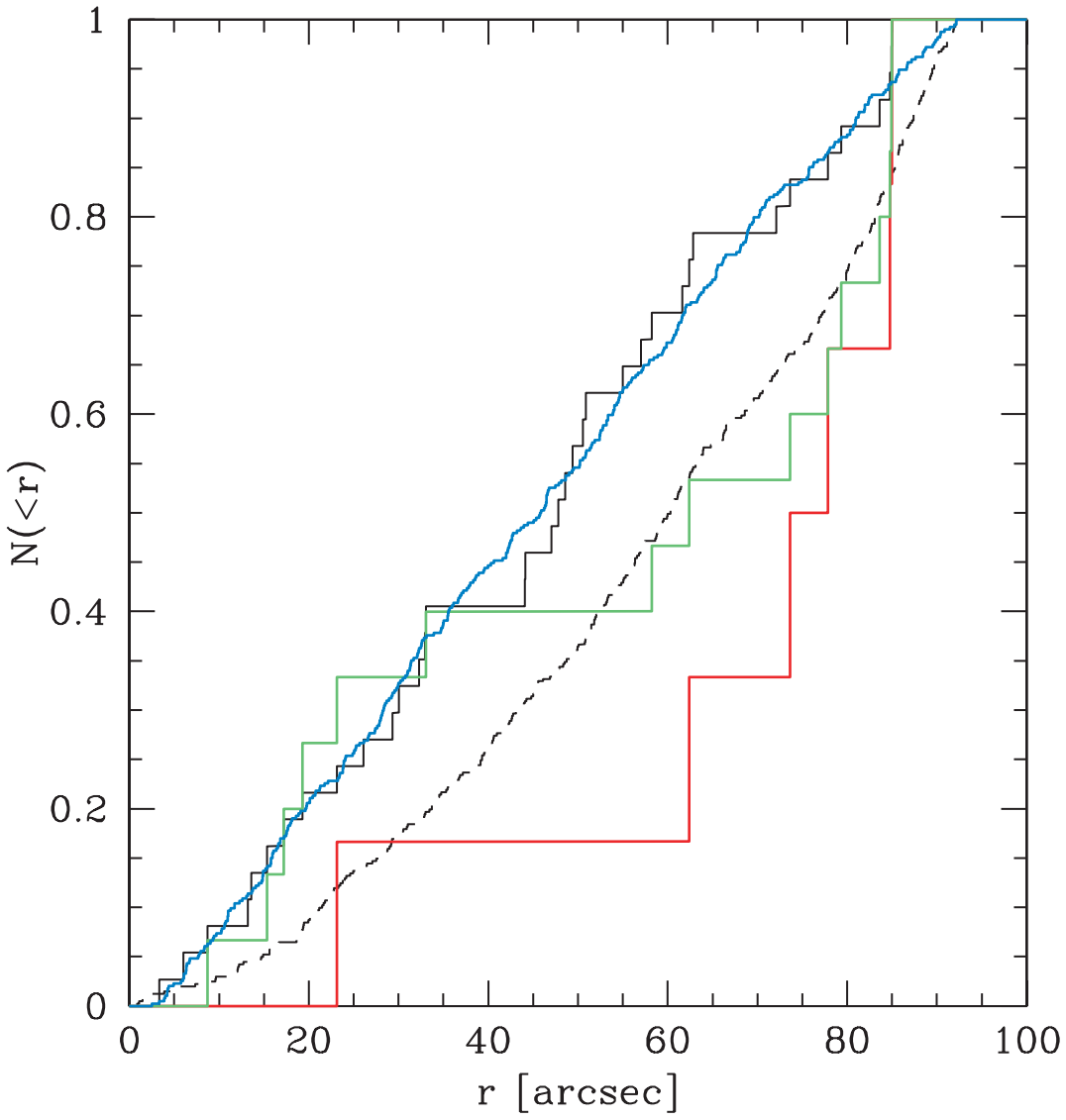

FIG. 8.—Cumulative radial distribution of objects in Abell 1689, restricted to the field of view of 92″ radius. *Blue histogram*: UCD candidates with $i > 27$ mag. *Black histogram*, UCD candidates with $i < 27$ mag; *green histogram*, UCD candidates with $i < 26$ mag; *red histogram*, UCD candidates with $i < 25$ mag; *dashed histogram*, dwarf galaxy candidates in Abell 1689 with $i < 26$ mag and $g - i > 1.1$ mag, taken from Infante et al. (2004).

with $i > 27$ mag in the color range of UCD candidates (GCS hereafter) is indicated. Note that the sample GCS contains the UCD candidates with 27 mag $< i <$ 28 mag and also all fainter sources and is therefore dominated by genuine globular clusters according to the results of § 3.3.

From Figure 8 it is evident that the UCDs with $i < 27$ mag are more strongly clustered than the two brighter subsamples and also the dE's. A Kolmogorov-Smirnov test shows that the cumulative radial distribution of UCD_1 is drawn from the same distribution as GCS at 97% confidence. The distribution of UCD_1 is inconsistent with that of the dE's at the 98% confidence level. This disagreement with the dE's drops to 53% for UCD_2 and 68% for UCD_3. UCD_1 is inconsistent with UCD_2 at 77%, and with UCD_3 at the 95% confidence level. For the six objects contained in UCD_3, no clustering is detectable.

These findings show that *only* for $i < 26$ mag ($M_V < -13.4$ mag), UCD candidates show a different radial distribution compared with the globular cluster system of Abell 1689. The fact that their distribution agrees better with that of the dwarf galaxies is consistent with the threshing scenario. Going back to the luminosity distribution of UCD candidates as shown in Figure 4, we found that in the magnitude range $26 < i < 26.8$, the predicted number of GCs from the best-fit GCLF is 4.3, while the number of UCD candidates is 12.1, inconsistent at the 2.2 σ level. For $i < 26$ mag, the disagreement is much stronger: only between zero and one GC is expected from the GCLF, compared with 10 objects actually found.

In conclusion, UCD candidates are well separated in luminosity and spatial distribution from GCs for $i < 26$ mag ($M_V < -13.4$ mag). For $i > 26$ ($M_V > -13.4$), our data suggest that genuine GCs are an important fraction. UCD candidates in that magnitude regime cannot be distinguished from GCs, and they might blend in with them. A minimum number of about 10 UCDs with $M_V < -13.4$ is then consistent with our results.

4. DISCUSSION

The aim of this section is twofold: first, to compare the expected number of stripped dE,N nuclei in Abell 1689 with the number of UCD candidates derived in the previous section;

second, to discuss several alternative possibilities for the identity of the very bright UCD candidates.

4.1. *Number of UCD Candidates*

Based on their simulations, Bekki et al. (2003) predict the number of UCDs expected from threshing dE,N's for the case of the Fornax and the Virgo Cluster. For Abell 1689 no such simulations yet exist. Abell 1689 has an X-ray temperature several times higher than Virgo (Young et al. 2002; Xue & Wu 2002) and about half as many spirals per E/S0 galaxy (Ferguson 1989; Balogh et al. 2002). However, the two clusters are similar in terms of enclosed mass and size, the two predominant factors that determine the number of UCDs expected from threshing dE,N's. While $M = 5 \times 10^{14}\ M_{\odot}$ and $M/L = 500$, with a scale radius $r_s = 226$ kpc for Virgo (Bekki et al. 2003), $M \simeq 1 \times 10^{15}\ M_{\odot}$ and $M/L \simeq 400$ with $r_s \simeq 350$ kpc for Abell 1689 (Broadhurst et al. 2004; King et al. 2002; Tyson & Fischer 1995). The mass value for Abell 1689 differs somewhat depending on the method used to derive it. The strong-lensing study of Broadhurst et al. obtains $\simeq 2 \times 10^{15}\ M_{\odot}$, and King et al. get $\simeq 5 \times 10^{14}\ M_{\odot}$ from weak gravitational lensing, while current X-ray estimates (Xue & Wu 2002; Andersson & Madejski 2004) yield lower results than the King et al. values by a factor of about 2.

For the Virgo Cluster, 46 UCDs are expected with a maximum projected radius of 700 kpc (Bekki et al. 2003). The number of UCDs and their radial extension should therefore be expected to be similar for Abell 1689. Note that for the Fornax Cluster, which has a mass almost 10 times smaller and a scale radius 3 times smaller, Bekki et al. predict 14 UCDs, in very good agreement with the number of UCD candidates found in Fornax by Mieske et al. (2004).

The maximum projected radius of the present investigation is about 285 kpc. According to Bekki et al.'s simulation for the Virgo Cluster, about 50% of UCDs created by threshing dE,N's are expected within this radius. Therefore, on the order of 20–25 UCDs should be found in the ACS image of Abell 1689. As shown in § 3.3, only for $i < 26$ mag ($M_V < -13.4$ mag) is it possible to reasonably estimate the number of UCD candidates, as their distribution is spatially more extended and they are brighter than expected for even the brightest GCs of Abell 1689's GCS. In that magnitude range, 10 UCD candidates are found. This number constitutes, of course, a lower limit on the number of UCDs. The overpopulation found for 26 mag $< i <$ 26.8 mag with respect to the GCLF would contribute another six to seven objects, but note that in this magnitude range the radial distribution of UCD candidates is indistinguishable from that of the GCs. Fainter than $i \simeq$ 26.8 mag, the majority of objects are GCs, but there can be UCDs mixing up with them.

In total, a number of 20–25 UCDs is consistent with our findings, which provide a lower limit of about 10 UCDs. Spectroscopic data for the (brightest) UCD candidates are necessary to definitely determine their cluster membership.

4.2. *Dwarf Galaxies Caught in the Act of Threshing?*

If all UCD candidates with $i < 26$ mag really were members of Abell 1689, this would imply that there are very bright UCDs reaching luminosities of $M_V \simeq -17.5$ mag ($i \simeq 22$ mag), almost 4 mag brighter than in Fornax. We might therefore see dwarf galaxies that are still in the process of disruption, being in the early stages of the threshing process as simulated by Bekki et al. (2003). The assumption that the UCD candidates originate from dwarf galaxies rather than globular clusters is supported by the fact that the very bright UCD candidates have a radial distribution that is more consistent with that of Abell 1689 dwarf galaxies than with the GCS. Moreover, the brightest UCD candidates are by far too luminous for globular clusters.

Another supportive finding is that the UCD candidates follow color-magnitude trends in both $g-i$ and $r-z$ (see Figs. 5 and 6) that place them redward of the dwarf galaxies. For the very bright UCD candidates with $i < 25.2$ mag, these relations are best defined. For $g-i$, the slope in that magnitude regime is -0.086 ± 0.012. The slope of the dwarf galaxy relation is -0.095, consistent with that of the UCD candidates. The mean color difference between the UCD and dwarf color-magnitude relation is 0.28 mag. Assuming that the UCD candidates are (partially) threshed dE,N's of unchanged color (see Mieske et al. 2004), that means that the UCD candidates are about $0.28/[(0.086 + 0.095)/2] \simeq 3$ mag fainter than their progenitors. In $r-z$, the UCD slope is -0.0315 ± 0.01, and the dwarf galaxy slope -0.068 ± 0.02, with the mean color difference between both relations being 0.092 mag. This implies a magnitude difference of $0.092/[(0.0315 + 0.068)/2] \simeq 2$ mag between UCD candidates and progenitor dE,N's.

These differences are smaller than the 4.1 mag difference between UCDs and progenitor dE,N's predicted by Bekki et al. (2003) and the difference of about 5 mag between dE,N's and their nuclei found observationally by Lotz et al. (2001). It therefore supports the hypothesis that the very bright UCD candidates are dE,N's that have not yet transformed entirely to naked nuclei, as also suggested from their higher luminosities as compared with the Fornax Cluster.

It is interesting to note that $M_V \simeq -17$ mag corresponds approximately to the total luminosity of M32, with M32's high surface brightness bulge being about 1 mag fainter (Mateo 1998; Graham 2002). The bulge component of M32 has an effective radius $r_{\rm eff}$ of about 100 pc (Faber et al. 1989; Graham 2002), which at the distance of Abell 1689 corresponds to about 0.″064 effective diameter. This angular size is about half of the PSF FWHM. An M32 A1689 equivalent, like the very bright UCD candidates, might therefore be marginally resolved. Figure 9 shows the six brightest UCD candidates ($i < 25$ mag) in the ACS image, with the same intensity cuts for each thumbnail. The two sources with 22.18 and 22.77 mag appear slightly more extended than the object with 22.38 mag. The SExtractor star classifier is 0.88 and 0.92 for the two more extended sources and between 0.93 and 0.98 for the other four. The differences become more evident in Figure 10. Here, the surface brightness profile of the three brightest and the faintest of the six objects is compared with the PSF profile of the ACS images. Evidently, the two sources with 22.18 and 22.77 mag have an extended envelope compared with the PSF profile. Comparing their brightness profile with convolved King profiles shows that a core radius of about 0.225 pixels—i.e., a core diameter and FWHM of 0.45 pixels, or 0.″0225—fits the observed profile best for both sources. This corresponds to a King profile core radius of about 35 pc at the distance of Abell 1689, several times larger than that found for the UCDs in Fornax (Drinkwater et al. 2003). The King profile can by definition not be characterized by an effective radius, as its integrated intensity rises proportionally to $\log r$ for large values of r. Therefore, in addition to the convolved King profiles, Figure 10 shows three convolved Sérsic profiles with Sérsic parameter $n = 2$. The curve corresponding to $r_{\rm eff} = 2$ pixels (0.″1) best fits the observed surface brightness of the two bright UCD candidates, yielding $r_{\rm eff} \simeq 310$ pc at the distance of Abell 1689. This

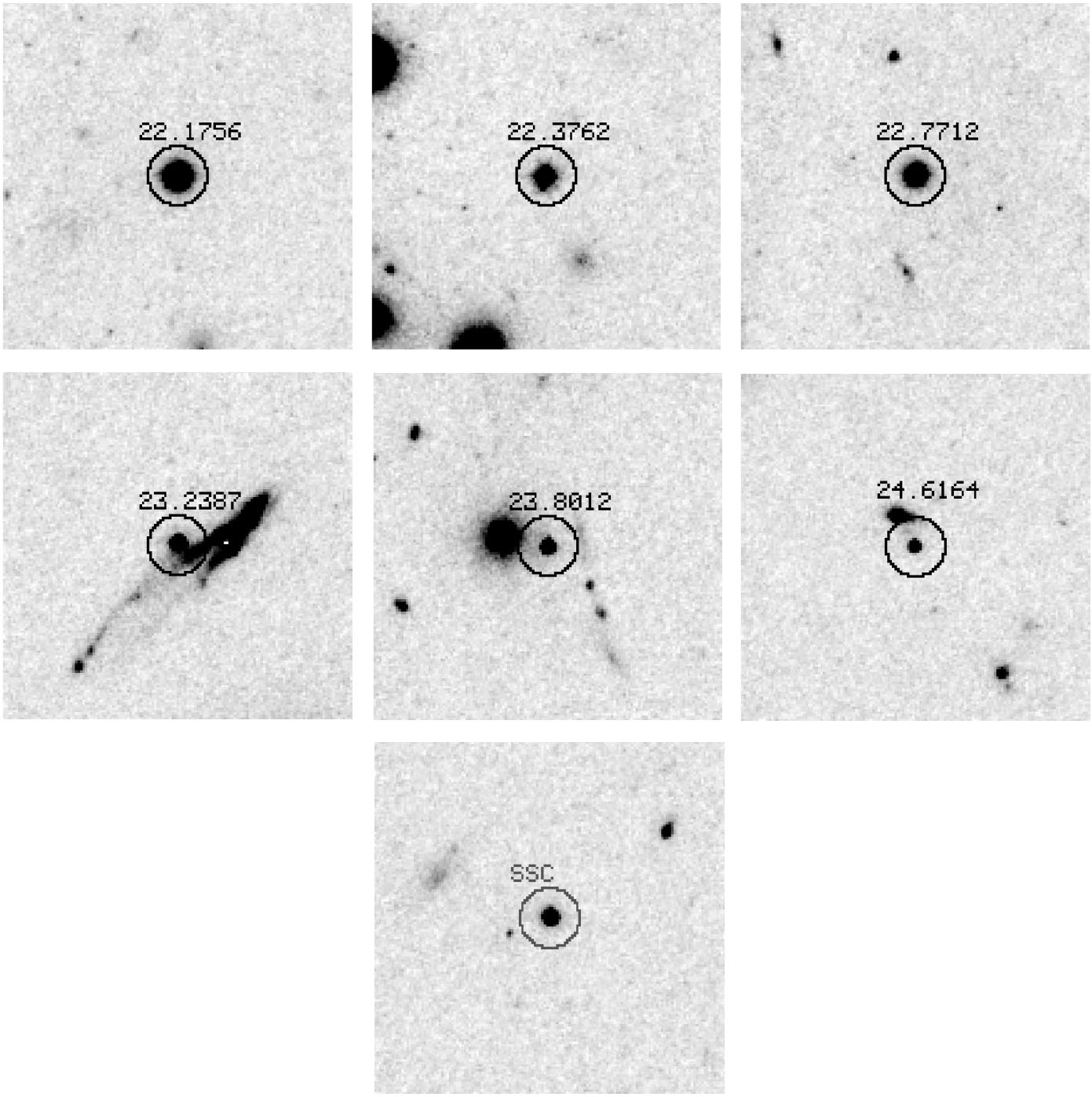

FIG. 9.—The $7'' \times 7''$ thumbnails of the six UCD candidates with $i < 25$ mag plus the one SSC candidate with $i \simeq 23.5$ mag; see text for details. The i magnitude is indicated for the UCD candidates. The two UCD candidates with 22.17 and 22.77 mag are slightly resolved; see Fig. 10 and text.

finding supports the hypothesis that these objects are dwarf galaxies *in the process of disruption* and therefore still possess to some degree a stellar envelope. Their spectroscopic confirmation as cluster members would further support the stripping hypothesis. A possible explanation for the still-ongoing stripping process might be that Abell 1689 consists of at least two subclusters separated in radial velocity (Teague et al. 1990; Girardi et al. 1997). This indicates that a merger process may be going on, possibly feeding the center of the cluster with ''fresh'' dwarf galaxies to be stripped.

Note that both the size and luminosity of the two resolved UCD candidates are a factor of 2–3 higher than those of M32's bulge (Graham 2002). It is therefore also possible that the latter objects are the bulges of stripped spiral galaxies, which is the favored origin for M32 by Graham's (2002) analysis of M32's surface brightness profile. This would imply the existence of a high surface brightness bulge—fitted well by a Sérsic profile with $n < 4$—and possibly an extended low surface brightness exponential disk. Given that the two UCD candidates are only marginally resolved, this is extremely difficult to check. From Figure 10 it is clear that a single Sérsic profile provides a good fit to the surface brightness profile of the two resolved UCDs. It is not necessary to include another component in the fit. Nevertheless, we cannot reject the possibility that the bright

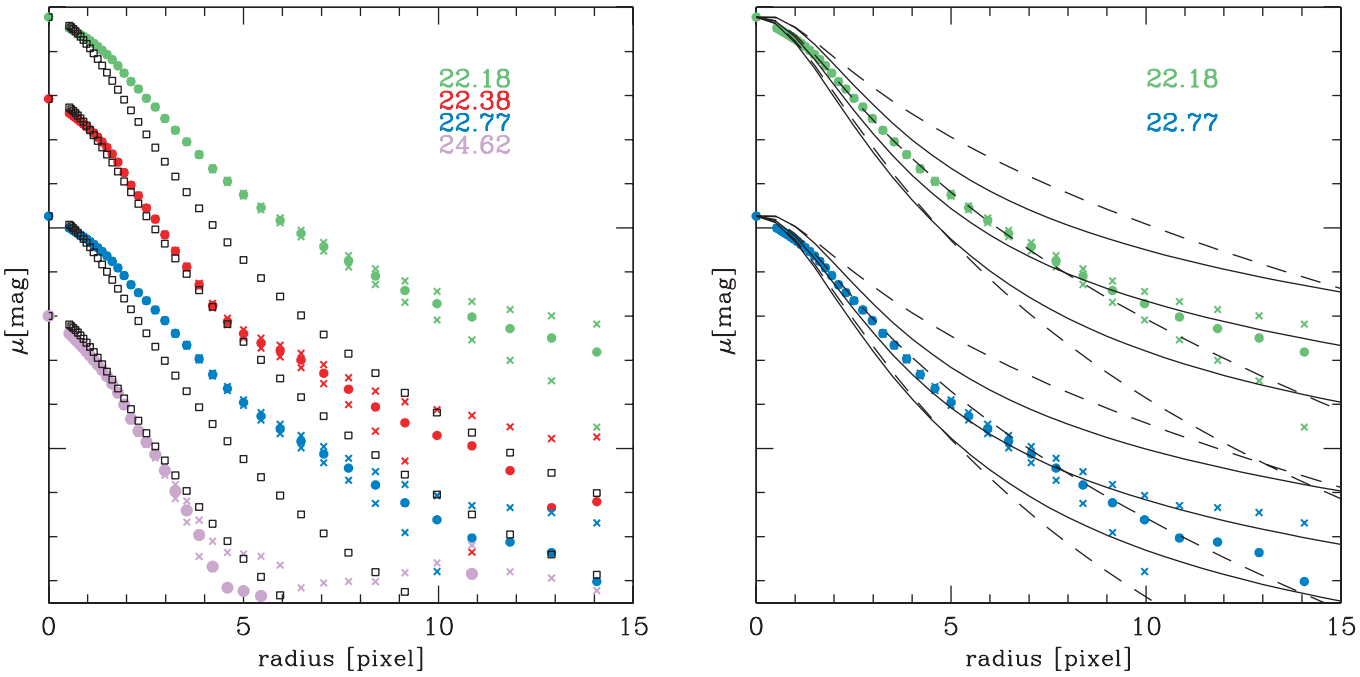

FIG. 10.—*Left*: Surface brightness profiles of four of the six very bright UCD candidates shown in Fig. 9, as measured on the detection image (the two missing UCD candidates have neighbors that are too close). The profiles have been scaled arbitrarily in order to avoid overlap and hence allow clearer distinction; one tick on the *y*-axis is 1 mag in surface brightness. The corresponding total magnitudes are indicated, allowing cross-identification with Fig. 9. Filled circles indicate the measured profile, and crosses indicate the result when adding and subtracting 1 sky standard deviation. Open squares indicate a Moffat profile with 0.″11 (2.2 pixels) FWHM (corresponding to the resolution of the image) with the same peak intensity as the respective object. Apparently, the two sources with 22.18 and 22.77 mag are slightly resolved. *Right*: Surface brightness profiles of the two resolved sources. The solid lines indicate King profiles with core radii of 0.45, 0.225, and 0.1125 pixels (*top to bottom*) convolved with the PSF and scaled to match the central intensity of the observed profile. The dashed lines are convolved Sérsic profiles with $n = 2$ and effective radii of 4, 2, and 1 pixels (*top to bottom*).

UCD candidates are bulges of stripped spirals, maybe with the outer exponential disk almost completely destroyed.

4.3. *Stellar Superclusters?*

The subclustering of Abell 1689 in radial velocity as mentioned in the previous section also opens up the possibility for an additional source of bright stellar clusters, as outlined by Fellhauer & Kroupa (2002). They show that in a merger process, very luminous stellar "superclusters" consisting of a large number of star clusters can be created, which after evolving dynamically and aging 10 Gyr resemble the properties of UCDs in Fornax. One existing example is W3 (Maraston et al. 2004), an extremely bright young supercluster in NGC 7252 of an age of about 300 Myr, which has $M_V \simeq -16$ mag. In the case of Abell 1689, the very bright UCD candidates may be very young superclusters. However, their color should be much bluer than that found here for Abell 1689. The color range of 1.3 mag $< g-i <$ 1.8 mag for the UCD candidates with $i < 25$ mag corresponds roughly to a rest-frame color of 1.0 mag $< V-I <$ 1.30 mag (see Fig. 1). Using Worthey (1994), the expected color for a stellar population of age 300 Myr is about $V-I = 0.6 \pm 0.1$ mag, depending on metallicity. Therefore, the very bright UCD candidates may not be "superclusters," unless they had initial masses near $10^9\ M_\odot$. Such large masses may be consistent with the Fellhauer & Kroupa scenario, which does not imply a fundamental physical upper mass limit for the hierarchical buildup of star cluster complexes, their masses being constrained by the available gas mass under high pressure. There are, however, three more unresolved sources at bluer colors than our UCD selection window see (Fig. 1). They have $i \simeq 23.5$ mag ($M_V \simeq -15.5$ mag) and $g-i \simeq 0.6$ mag, which is on the order of what would be expected for SSCs. However, for two of these three, the photometric redshift is 0.01, consistent with their being either foreground stars or intergalactic globular clusters. For the third object (the reddest one), the photometric redshift is 0.25 ± 0.08, consistent with that of the cluster. (See Fig. 9 for a thumbnail.)

Hence, we might have found one analog to W3 in Abell 1689 at a bluer color than the UCD candidates. Spectroscopic measurements are necessary to prove this assumption.

4.4. *Foreground Stars?*

Another possibility for the origin of the very bright UCD candidates is that some of them are foreground stars located in the Milky Way or its halo, especially the four that are definitively unresolved. The color range of the very bright UCD candidates of 1.3 mag $< V-I <$ 1.55 mag corresponds to K- and M-type subdwarfs (Gizis & Reid 1999). The absolute brightness of these subdwarfs is about $M_V \simeq 9$ mag, corresponding to a distance of about 10 kpc if the very bright UCD candidates actually are subdwarfs. The very bright UCD candidates extend about 3 mag in luminosity, or a factor of about 4 in distance if interpreted as subdwarfs with identical absolute luminosity. This means they would occupy the distance range 5–20 kpc. The field of view of the ACS ($3' \times 3'$) corresponds to about 9 pc $\times$ 9 pc at 10 kpc distance. This translates into a volume of about 10^6 pc^3. The space density of halo stars at a distance of 10 kpc is about 10^{-6} pc^{-3} (Kerber et al. 2001; Phleps et al. 2000). This shows that some of the very bright UCD candidates could be halo subdwarfs.

However, note that the mean photometric redshift of the six very bright UCD candidates is 0.245 ± 0.06, consistent with that of the cluster. These photometric redshifts, as is true for all those quoted in this paper, were calculated using the Bayesian

TABLE 1
PHOTOMETRIC REDSHIFTS z_{phot} FOR THE SIX BRIGHTEST UCD CANDIDATES[a]

Candidate	i (mag)	$z_{phot,star}$ (χ^2)	$z_{phot,ell}$ (χ^2)	$z_{phot,all}$ (χ^2)
1	22.18	0.091 ± 0.073 (7.9)	0.164 ± 0.078 (3.9)	0.160 ± 0.076 (7.1)
2	22.38	0.001 ± 0.067 (2.6)	0.188 ± 0.079 (16.1)	0.300 ± 0.076 (18.9)
3	22.77	0.102 ± 0.029 (8.8)	0.180 ± 0.079 (5.0)	0.180 ± 0.078 (5.0)
4	23.24	0.001 ± 0.067 (47.2)	0.001 ± 0.067 (18.35)	0.090 ± 0.072 (12.8)
5	23.80	0.001 ± 0.069 (3.3)	0.142 ± 0.076 (13)	0.250 ± 0.085 (18)
6	24.62	0.001 ± 0.067 (24.7)	0.001 ± 0.067 (35)	0.490 ± 0.098 (36)

[a] Obtained in three different ways: $z_{phot,star}$ from using stellar templates of K- and M-type subdwarfs without prior probabilities; $z_{phot,ell}$ from using the elliptical galaxy template of Benítez (2004), also without priors; and finally, $z_{phot,all}$ from using the entire set of six different galaxy-type templates with prior probabilities (see Coe et al. 2004; Broadhurst et al. 2004). Errors are 1 σ. The χ^2 values show how well the template and object colors match at the calculated photometric redshift.

photometric redshifts (BPZ) code by Benítez (2000). This involves the assignment of redshift-dependent prior probabilities to six different galaxy templates ranging from an elliptical to an irregular galaxy SED. It is clear that for the six brightest UCD candidates, a statistical approach like the Bayesian one might not be very reliable anymore. Some of the template SEDs used in the BPZ algorithm—probably the late-type ones—may not match very well the expected SED of an UCD. Therefore, we calculate the photometric redshift of the six very bright UCD candidates in two additional ways, using the BPZ code: First, we use only the stellar templates of K- and M-type subdwarfs from Pickles (1998) without prior probabilities. This is done to see how many UCD candidates have colors consistent with foreground stars. Second, we use the elliptical template from Benítez et al. (2004), also without prior probabilities. UCDs are supposed to be early-type stellar populations, and hence an elliptical galaxy template should be a good approximation of a real UCD spectrum. Note that up to now, no precise age/metallicity or line index measurements of UCDs have been published.

The results of the calculations are shown in Table 1, indicating the photometric redshifts, their errors, and the χ^2 of the redshift determination. The results can be summarized as follows: The two slightly resolved candidates 1 and 3 are the only ones that are inconsistent with stars at $z_{phot} = 0$ and match the redshift $z = 0.183$ of Abell 1689 from $z_{phot,ell}$ and $z_{phot,all}$. Candidate 2 is more consistent with a star at $z_{phot} = 0$ than with an early-type stellar population in Abell 1689. Candidate 4 is marginally inconsistent with Abell 1689 from $z_{phot,all}$ and more likely to be an early-type stellar population at lower redshift, possibly an intergalactic globular cluster. Comparing the χ^2 values, we find it less likely that it is a foreground star. Candidate 5 is consistent with a star at $z_{phot} = 0$, while both $z_{phot,ell}$ and $z_{phot,all}$ attribute it to Abell 1689's redshift. The χ^2 value is lower for the stellar template, and hence this candidate has an ambiguous redshift assignment with slight preference for a foreground star. Candidate 6's $z_{phot,all}$ is very high, at the upper limit of that adopted in this paper as a possible photometric redshift for Abell 1689 members. At the same time, it is consistent with a star at $z_{phot} = 0$ and an early-type population at low redshift, with slightly lower χ^2 for the star possibility. It seems that candidate 6 is therefore either a foreground star or an intergalactic globular cluster.

In summary, UCD candidates 1 and 3 are the least probable foreground stars and most probable cluster members out of the six candidates, because of their resolved morphology and their photometric redshifts. For candidates 2, 4, 5, and 6, the photometric redshift information is more ambiguous and does not allow a clear assignment. Among them, candidate 6 is the least probable cluster member.

It is therefore concluded that there are up to four foreground stars among the six brightest UCD candidates, with the corresponding number of Abell 1689 members being between five and two. Spectroscopic membership confirmation is needed for more specific statements.

4.5. *Background or Foreground Galaxies?*

Another clear possibility for the identity of the brightest UCD candidates is that they are galaxies or globular clusters that are not members of Abell 1689. The field of view toward Abell 1689 in the investigated color range is dominated by cluster members, but as we consider only six objects, statistical fluctuations might cause a substantial fraction of these six objects to be in front of or behind the cluster. With the photometric redshifts listed in Table 1, it is clear that candidates 2, 4, and 6 have either $z_{phot,ell}$ or $z_{phot,all}$ inconsistent with the redshift of Abell 1689. Among these, candidate 4 is most likely to be a foreground object, most possibly an intergalactic globular cluster. Candidate 2 could be a background galaxy, but note that its $z_{phot,all}$ is less than 2 σ away from the redshift of Abell 1689. Candidate 6 has very low $z_{phot,ell}$ and very high $z_{phot,all}$ at comparable χ^2. For this object, the question whether its colors are created by intrinsically red populations at low redshift or blue populations at higher redshift cannot be answered with certainty.

In conclusion, among the six very bright UCD candidates there are three probable or possible noncluster and nonstellar objects: one probable foreground globular cluster, one possible background galaxy, and one probable noncluster member, which can be either foreground or background.

5. SUMMARY AND CONCLUSIONS

In this paper, the distribution in color, magnitude, and space of ultracompact dwarf galaxy candidates (Mieske et al. 2004; Drinkwater et al. 2003) in the central 92″ (285 kpc) of Abell 1689 ($z = 0.183$, $m - M = 39.74$ mag) has been investigated. The UCD candidates were selected from deep ACS images in *griz*, based on their magnitude ($i < 28$ or $M_V < -11.5$ mag), size (unresolved), and color. The color windows were 1.2 mag $< g-i <$ 1.8 mag and 0.38 mag $< r-z <$ 0.73 mag, defined with the Bayesian photometric redshift code BPZ by Benítez (2000). There are 160 UCD candidates in Abell 1689 with 22 mag $< i <$ 28 mag. Combining photometric redshifts and the radial density distribution of the UCD candidates shows that about 100 of the 160 UCD candidates are cluster

members. In the investigation of their properties, the following results are obtained:

1. The UCD candidates extend to $M_V \simeq -17.5$ mag, about 4 mag brighter than in the Fornax Cluster. Their luminosity distribution for 26.8 mag $< i <$ 28 mag ($-12.7 < M_V < -11.5$) is approximated well by the bright end of a Gaussian globular cluster luminosity function shifted to Abell 1689's distance, implying a total number of about $(3-10) \times 10^4$ GCs. For $i < 26.8$ mag, the UCD candidates define an overpopulation with respect to the GCLF of about a factor of 4, as 20 objects are discovered when about five are predicted. This overpopulation is on the order of the number of UCDs expected from the threshing scenario (Bekki et al. 2003) in Abell 1689.
2. The UCD candidates follow a color-magnitude trend with a slope similar to that defined by the genuine dwarf galaxies in Abell 1689, but shifted somewhat redder. The shift between the two relations corresponds to a magnitude difference of 2–3 mag, about 1–2 mag less than what is expected for the difference between parent dwarf galaxy and stripped nucleus from the simulations of Bekki et al. (2003).
3. The radial distribution of UCD candidates with $i > 27$ mag is consistent with that of the GC system. For $i > 26$ mag it is shallower and more consistent with that of the genuine dwarf galaxy population in Abell 1689.
4. Two of the three brightest UCD candidates with $M_V \simeq -17$ mag are slightly resolved on the ACS images, with implied King profile core radii of 35 pc and effective radii of about 300 pc at the distance of Abell 1689. These sizes and luminosities are about 2–3 times higher than the values found for M32's bulge by Graham (2002).
5. Photometric redshifts obtained with late-type stellar templates and an elliptical galaxy template support the assignment of the two resolved UCD candidates to Abell 1689 based on the original Bayesian photometric redshift calculation. However, they also allow for up to four foreground stars among the six brightest UCD candidates.
6. There are three SSC candidates (Fellhauer & Kroupa 2002) with $M_V \simeq -16$ mag, substantially bluer than the UCD candidates.

All our findings are consistent with the threshing scenario (Bekki et al. 2003) as a source of at least 10 UCDs for $i <$ 26.8 mag ($M_V < -12.7$ mag). UCD galaxies created by stripping "normal" dwarf or spiral galaxies appear to exist in Abell 1689. For $i > 26.8$, the globular cluster population of Abell 1689 clearly dominates over possible UCDs created by threshing. For the following reasons, it appears likely that in the case of Abell 1689 the threshing process has not yet finished: (1) the UCD candidates extend to about 4 mag brighter than in Fornax; (2) their colors are closer to those of genuine dE's than in Fornax; and (3) two of the three brightest UCD candidates are resolved, implying sizes several times larger than for the UCDs in Fornax.

The next step is clear: spectroscopic confirmation of the cluster membership assignment obtained with photometric redshifts for the UCD candidates in this paper. For the very brightest UCD candidates with 22 mag $< i <$ 24 mag, this should be a feasible task with an 8 m class telescope. The spectroscopic confirmation would prove the existence of ultracompact dwarf galaxies at almost 50 times the distance of the Fornax Cluster, the location of the UCD's original discovery. It would imply that the disruption of dwarf or spiral galaxies in the cluster tides may be a common process. Detailed numerical simulations to test the magnitude of this effect for fainter luminosities are needed. These would allow us to check the extent to which tidal disruption might be responsible for the "missing satellite" problem, i.e., the disagreement between the predicted and observed frequency of dark matter halos.

ACS was developed under NASA contract NAS 5-32864, and this research has been partially supported by NASA grant NAG 5-7697 and by an equipment grant from Sun Microsystems, Inc. The Space Telescope Science Institute is operated by the Association of Universities for Research in Astronomy, Inc., under NASA contract NAS 5-26555. We are grateful to K. Anderson, J. McCann, S. Busching, A. Framarini, S. Barkhouser, and T. Allen for their invaluable contributions to the ACS project at Johns Hopkins University. S. M. was supported by DAAD Ph.D. grant D/01/35298 and DFG Projekt HI 855/1-1. L. I. would like to acknowledge support from Proyecto Fondap M. S. thanks the ESA RSSD 15010003.

REFERENCES

Andersson, K. E., & Madejski, G. M. 2004, ApJ, 607, 190
Balogh, M. L., Couch, W. J., Smail, I., Bower, R. G., & Glazebrook, K. 2002, MNRAS, 335, 10
Bekki, K., Couch, W. J., Drinkwater, M. J., & Shioya, Y. 2003, MNRAS, 344, 399
Benítez, N. 2000, ApJ, 536, 571
Benítez, N., et al. 2004, ApJS, 150, 1
Bertin, E., & Arnouts, S. 1996, A&AS, 117, 393
Blakeslee, J. P. 1999, AJ, 118, 1506
Blakeslee, J. P., Meurer, G. R., Ford, H. C., Benítez, N., White, R. L., Zekser, K. C., & Sirianni, M. 2004, Highlights Astron., 13, in press
Broadhurst, T., et al. 2004, ApJ, submitted
Coe, D. A., et al. 2004, in preparation
Dirsch, B., et al. 2003, AJ, 125, 1908
Drinkwater, M. J., Gregg, M. D., Hilker, M., Bekki, K., Couch, W. J., Ferguson, H. C., Jones, J. B., & Phillipps, S. 2003, Nature, 423, 519
Drinkwater, M. J., Jones, J. B., Gregg, M. D., & Phillipps, S. 2000, Publ. Astron. Soc. Australia, 17, 227
Duc, P.-A., et al. 2002, A&A, 382, 60
Faber, S. M., et al. 1989, ApJS, 69, 763
Fellhauer, M., & Kroupa, P. 2002, MNRAS, 330, 642
Ferguson, H. C. 1989, Ap&SS, 157, 227
Fukugita, M., et al. 1996, AJ, 111, 1748
Girardi, M., et al. 1997, ApJ, 490, 56
Gizis, J. E., & Reid, I. N. 1999, AJ, 117, 508
Graham, A. W. 2002, ApJ, 568, L13 (erratum 572, L121)
Hilker, M., Mieske, S., & Infante, L. 2003, A&A, 397, L9
Infante, L., et al. 2004, in preparation
Kerber, L. O., Javiel, S. C., & Santiago, B. X. 2001, A&A, 365, 424
King, L. J., Clowe, D. I., & Schneider, P. 2002, A&A, 383, 118
Klypin, A., Kravtsov, A. V., Valenzuela, O., & Prada, F. 1999, ApJ, 522, 82
Kroupa, P. 1998, MNRAS, 300, 200
Kundu, A., & Whitmore, B. C. 2001, AJ, 121, 2950
Lotz, J. M., et al. 2001, ApJ, 552, 572
Maraston, C., et al. 2004, A&A, 416, 467
Mateo, M. 1998, ARA&A, 36, 435
Mieske, S., Hilker, M., & Infante, L. 2002, A&A, 383, 823
———. 2004, A&A, 418, 445
Moore, B., et al. 1999, ApJ, 524, L19
Phleps, S., Meisenheimer, K., Fuchs, B., & Wolf, C. 2000, A&A, 356, 108
Pickles, A. J. 1998, PASP, 110, 863
Sirianni, M., et al. 2004, in preparation
Teague, P. F., Carter, D., & Gray, P. M. 1990, ApJS, 72, 715
Tyson, J. A., & Fischer, P. 1995, ApJ, 446, L55
Worthey, G. 1994, ApJS, 95, 107
Xue, S., & Wu, X. 2002, ApJ, 576, 152
Young, A. J., & Wilson, A. S. 2002, ApJ, 579, 560
Zekser, K. C., et al. 2004, in preparation